Materials Science-Poland, 40(3), 2022, pp. 72-79
http://www.materialsscience.pwr.wroc.pl/
DOI: 10.2478/msp-2022-0032

Tailoring hydrophobicity properties of polyvinylidene fluoride infused graphene composite films

Ab Rahman Marlinda[1,*], Yusliza Yusof[1], Nurul Azri Khalisah Aznan[1], Nurafaliana Berahim[1], Nor Aliya Hamizi[1], Leo Bey Fen[2], Raja Amin Raja Mokhtar[2], Mohd Rafie Johan[1]

[1]Institute for Advanced Studies, University of Malaya, Nanotechnology & Catalysis Research Centre (NANOCAT)
[2]Department of Surgery, Faculty of Medicine, University of Malaya, 50603, Kuala Lumpur, Malaysia

In this work, a synthesis to improve surface wetting resistance composites via infusion of graphene (G) structure into the polyvinylidene fluoride (PVDF) matrices is introduced. Graphene is incorporated into the PVDF matrix with a percentage of 1.0 wt.% up to 2.5 wt.% using simple solvent blending and dry-casting methods. The morphological and structural properties of the graphene infused into PVDF are investigated using a variety of characterization techniques, including field emission scanning electron microscopy, energy-dispersive X-ray spectroscopy (EDX), and Raman spectroscopy. The tensile properties of graphene infused into the PVDF matrix are investigated using the INSTRON Universal test. The need for hydrophobicity performance on polyvinylidene fluoride infused graphene (PVDF/G) composite is also reported. Based on our evaluation, we ascertain that the PVDF/G-1.5% produces extremely high values for ultimate tensile stress and Young's modulus, amounting, respectively, to 90.24 MPa and 5720.88 MPa. The PVDF/G composite exhibits surface roughness and increases water contact angle (CA) by 20° more than pure PVDF. Therefore, it is possible to deploy PVDF/G composite thin films with suitable mechanical strength and hydrophobicity in biomedical material-based engineering applications.

Keywords: *graphene, PVDF, mechanical properties, hydrophobic, microscopy*

1. Introduction

Poly(vinylidene fluoride) or polyvinylidene difluoride, one of the high thermoplastic polymers, is a semicrystalline material that is usually produced through polymerization of vinylidene difluoride. Polyvinylidene fluoride (PVDF) has many excellent combination properties, including high chemical resistance [1], remarkable mechanical strength [1], remarkable flame retardation [2], good processability [3], excellent mechanical flexibility [4], good piezoelectric properties [5], and efficiency in terms of piezoelectricity [6] and pyroelectricity [7]. It is a naturally good hydrophobic material that can retain air at the solid–liquid interface when in contact with water. The high hydrophobicity of PVDF could reduce surface roughness and water contact angle (CA) since the dense skin layer formation on a material surface is greatly influenced by its wettability properties [8], high hydrophilicity, and excellent underwater superoleophobicity [9]. It also has low permeability to most gases and liquids and for this reason is available as a recycled polymer that can be used in the long term. Since its discovery in 1969 by Dr. Heijji Kawai [10], it has been commonly implemented in many application areas such as electronics, actuators, chemical processing equipment, and biomedical because of its unique properties.

The biomedical applications of polymeric materials are due to their versatility in chemical groups and carbon-based chemical structures that are most likely to be characterized by a close cohesion with biological tissues' mechanics. In modern medicine, synthetic organic polymers play a significant role in treating medical conditions either for temporary in-vivo applications or general surgical implants. Many polymers are desirable as biomaterials that can interact directly with human tissues and organs. However, body tissues with biomaterial surfaces may cause problems stemming from the polymer material being treated as a foreign body, which

* E-mail: drmarlinda2205@gmail.com

© Ab Rahman Marlinda et al. 2022. This is an open access article distributed under the Creative Commons Attribution-NonCommercial-NoDerivatives 4.0 License. (http://creativecommons.org/licenses/by-nc-nd/4.0/)

might give rise to complications such as blood coagulation and a hostile immune response. Thus, the composition and architecture of the synthetic, engineered materials vary according to tissue types and individual tissues. The most crucial aspect is the one pertaining to the chronological age and the progress of the disease. For example, large blood vessels [11], gross arterial stiffness [12], and increased cardiovascular disease end points including stroke [13], chronic kidney [14], and abdominal aortic aneurysm [15] are primary risk factors. Besides that, increased blood pressure [16], diabetes mellitus [17], glucose intolerance [18], and end-stage renal failure [19] are other pathologic entities associated with increased cardiovascular risk due to failure on arterial stiffness.

Fast development in innovative application areas, such as smart materials, and self-cleaning and anti-sticking coatings, has led to extremely high demand for the production of superhydrophobic and superoleophobic-based materials. Thus, one of the essential properties of these superhydrophobic and superoleophobic materials is excellent liquid wettability that demonstrates a low collaboration surface energy compound and the combination of micro- and nano-scaled surfaces. Among the organic polymers, PVDF and its composites constitute the focus of this study since the polymer itself has been widely used in medical applications. PVDF has been used in general surgery as the synthetic non-resorbable suture material for tissues, such as skin or tendons, which are exposed to high mechanical forces and whose healing processes are therefore constrained by a slow rate of progress [20]. Alternatively, PVDF thin film can be proposed as an ideal biomaterial coating embedded within the biological tissue. Besides, the hydrophobic surface of PVDF is an advantage in that it provides water repellency and a self-cleaning surface at the biomaterial–water interfaces, thereby debarring access to any debris and pathogens. The PVDF film also can be utilized as substrates to control protein adsorption [21], cellular interaction, and bacterial growth [22].

Meanwhile, given the background of the need for tailoring the surface morphology of PVDF composites in a way that would effectively improve their hydrophobicity properties, significant interest has been aroused in incorporating carbon-based materials such as nanotubes (CNTs) and graphene into nanostructure materials. Among all carbon-based materials, graphene continuously attracts a significant amount of attention from the research community, as nano-sized fillers possess a high aspect ratio and low mass density. As a result of the dedicated efforts directed toward the production of functional and structural polyvinylidene fluoride infused graphene (PVDF/G), it has become possible to obtain improved composites with promising mechanical performance [23] and hydrophobic surfaces [24].

This article purposely focused on a few crucial characteristics that need to be considered in synthesizing materials for biomedical purposes and is organized as follows: First, the mechanical properties of PVDF/G composite thin films with different graphene loadings are discussed. Second, the structural properties and surface morphology of the PVDF/G composites are investigated using Raman spectra. Third, the infusion effect of graphene on the hydrophobic properties of the PVDF/G composite is presented and discussed.

2. Material and methods

2.1. Materials

All chemicals are of analytical reagent grade and used as received. PVDF (MW ~534,000 by GPC, powder) and dimethylformamide (DMF, anhydrous 99.8%) were purchased from Sigma Aldrich, Inc. (St. Louis, USA).

2.2. Preparation of PVDF/G composites

The graphene dispersion was obtained in DMF solvent (1 mg·mL^{-1}) by ultra-sonicated graphene powder for 2 h at a temperature <60°C. This temperature was chosen since the flashpoint of DMF is ~60°C. Meanwhile, 2.0 g of PVDF powder was prepared separately in 30 mL of DMF solvent. The PVDF dispersion was obtained after a 2 h magnetic stirring at 30°C. A graphene-DMF dispersion with different graphene loading ranges (1.0 wt.%, 1.5 wt.%, 2.0 wt.%, and 2.5 wt.%) was slowly mixed

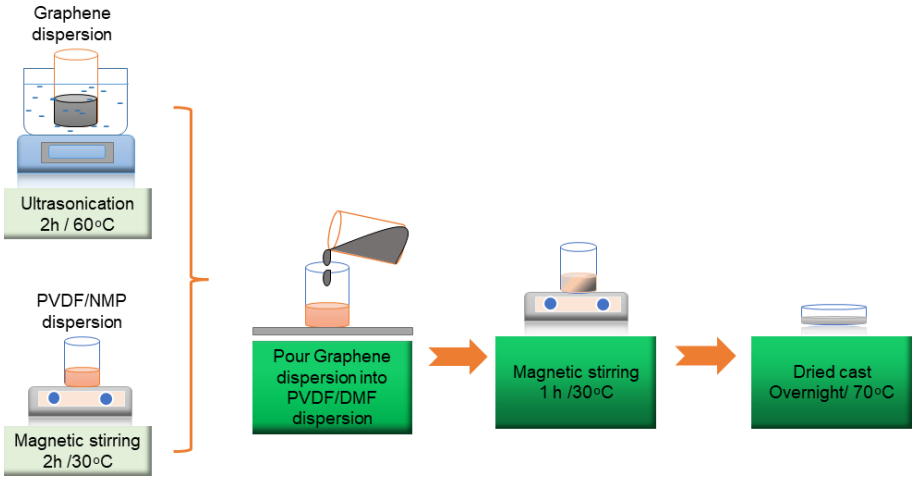


Fig. 1. A schematic illustration for the synthesis of PVDF/G composite film. PVDF, polyvinylidene fluoride; PVDF/G, polyvinylidene fluoride infused graphene

into the PVDF/DMF dispersion. A well-dispersed PVDF incorporated graphene was obtained after 5 min of ultrasonication.

Additionally, the mixed solution was continuously stirred at 500 rpm at 60°C for 1 h to allow the interaction to occur for good dispersion of the composite. Then, the homogeneous solution was dried-cast on a glass substrate using a film casting knife technique. The composite film was dried in a vacuum oven at 70°C overnight to evaporate the solvent. Finally, the end-product was obtained as a thin film composite with an average thickness of 150 μm. Figure 1 illustrates a schematic for the synthesis of PVDF/G composite film.

2.3. Characterizations

The PVDF/G composite morphology was observed using field emission scanning electron microscopy (SEM; Quanta 200 FESEM, FEI, Eindhoven, Netherlands) operated at 10.0 kV. The energy-dispersive X-ray spectroscopy (FEI, Eindhoven, Netherlands) was utilized to study the elemental mapping of the PVDF/G composite film. Meanwhile, the PVDF/G composite's structural properties were characterized using inVia Raman Microscope spectroscopy (Renishaw, Gloucestershire, UK) using 532 nm laser-excitation. The mechanical tensile properties of the samples were analyzed using a universal testing machine, INSTRON 3300-100kN (Norwood, USA), with film of $<$1 mm thickness as per ASTM D882. Specimen samples with dimensions of 20 mm in width and 80 mm in length were used for performing mechanical tensile tests at a strain rate of 100 mm·min^{-1}. Using an optical tensiometer (DYNE Technology, Staffordshire, UK) equipped with a micro-syringe, water CA measurements were carried out. A water droplet volume of 2 μL was deposited onto the film surface from a distance of 5 cm and left for 60 s before the image was captured.

3. Results and discussion

3.1. Tensile properties

A mechanical tensile test is performed to investigate the suitability of the PVDF and its composites for serving as a substrate from which to develop an ideal biomaterial. Table 1 compares the uniaxial tensile properties of the native heart valves, blood vessels, PVDF, and PVDF/G composites with different graphene loading ratios. The PVDF/G composite with an increment of graphene content shows an increase in ultimate tensile stress up to 1.5 wt.% of graphene content from the tabulated data. Later, the ultimate tensile stress obtained is decreasing when the graphene percentage is increased. The PVDF/G-1.5 wt.% displays extremely high ultimate tensile stress and Young's modulus

Table 1. A comparison of uniaxial tensile properties of native heart valves, blood vessels, PVDF, and PVDF-G composites

Samples (thickness ~15 mm)	Ultimate tensile strength, σ (MPa)	Strain, ε (%)	Young's modulus, E (MPa)
Human aortic valve [28]	2.60	22.00	15.00
Porcine aortic valve [29]	1.30	10.80	7.80
Blood vessel [30]	0.20–0.60	-	2.00–6.00
PVDF	23.40	69.30	417.64
PVDF/G-1.0 wt.%	19.29	4.68	492.64
PVDF/G-1.5 wt.%	90.24	2.30	5,720.88
PVDF/G-2.0 wt.%	56.59	3.67	2,740.64

PVDF, polyvinylidene fluoride; PVDF/G, polyvinylidene fluoride infused graphene

values, amounting, respectively, to 90.24 MPa and 5720.88 MPa. These remarkable values might be contributed by the strong interaction between the graphene and PVDF [25], where the graphene acts as a nanofiller with a high specific surface area, able to withstand external forces better than pure PVDF [26]. However, with further increases in graphene percentages up to 2.0 wt.% of graphene loading, the ultimate tensile stress and Young's modulus values are decreased. One potential explanation for this phenomenon, which was put forward in the study of Francis et al. [27], is that increasing graphene loading restricts the movement of PVDF polymer chains, which leads to poor tensile properties. Thus, the outcomes indicate that 1.5 wt.% of graphene loading is the optimum amount to enhance the tensile stress. This well distributed rigid network of graphene filler can carry most of the applied load, resulting in better mechanical properties.

Figure 2 shows that the composites' ultimate strength and Young's modulus (E) were significantly increased at 1.5 wt.% of graphene. However, the strain value of the composite was reduced to 2.3%. In contrast, pure PVDF (refer to Table 1) shows lower strength and large elongation, which indicates a significant plastic deformation before failure. The high strain is not favorable because it may lead to calcification of the heart valve. However, the physiological conditions in vivo can be characterized further by fatigue or bending stress. As seen in Table 1, the highest values of ultimate tensile strength and modulus of elasticity that can be attained while still retaining the original shape

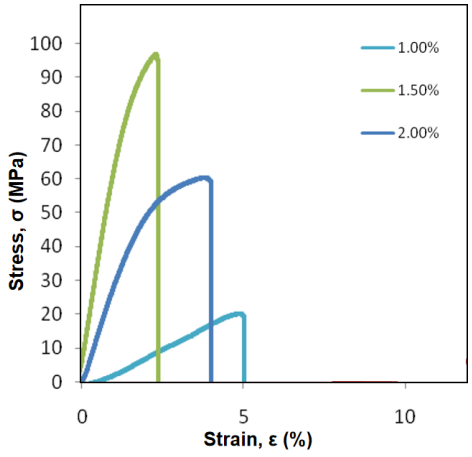


Fig. 2. Stress (MPa) versus strain (%) of PVDF/G composites. PVDF/G, polyvinylidene fluoride infused graphene

are obtained for PVDF/G-1.5 wt.%.The PVDF/G-1.5 wt.% curve exhibits a sharp rise in tensile stress with a little strain value, likely to imitate standard native heart valve leaflets' behavior. Human leaflet thickness ranged from 177 μm to 1.76 μm in a relaxed state, while 150 μm to 1.75 μm is the range observed corresponding to a stressed state [30]. Meanwhile, the PVDF/G-1.0 wt.% exhibits lower ultimate tensile strength compared to PVDF/G-1.5 wt.%, but is higher in strain percentage, almost at 5%. However, an increase in graphene loading up to 2.0 wt.% shows significant decreases in ultimate tensile strength at an extended elongation strain of >3%. It can be explained that at a 2.0 wt.% loading of the graphene filler, the graphene aggregation in the network interaction within the PVDF matrix is

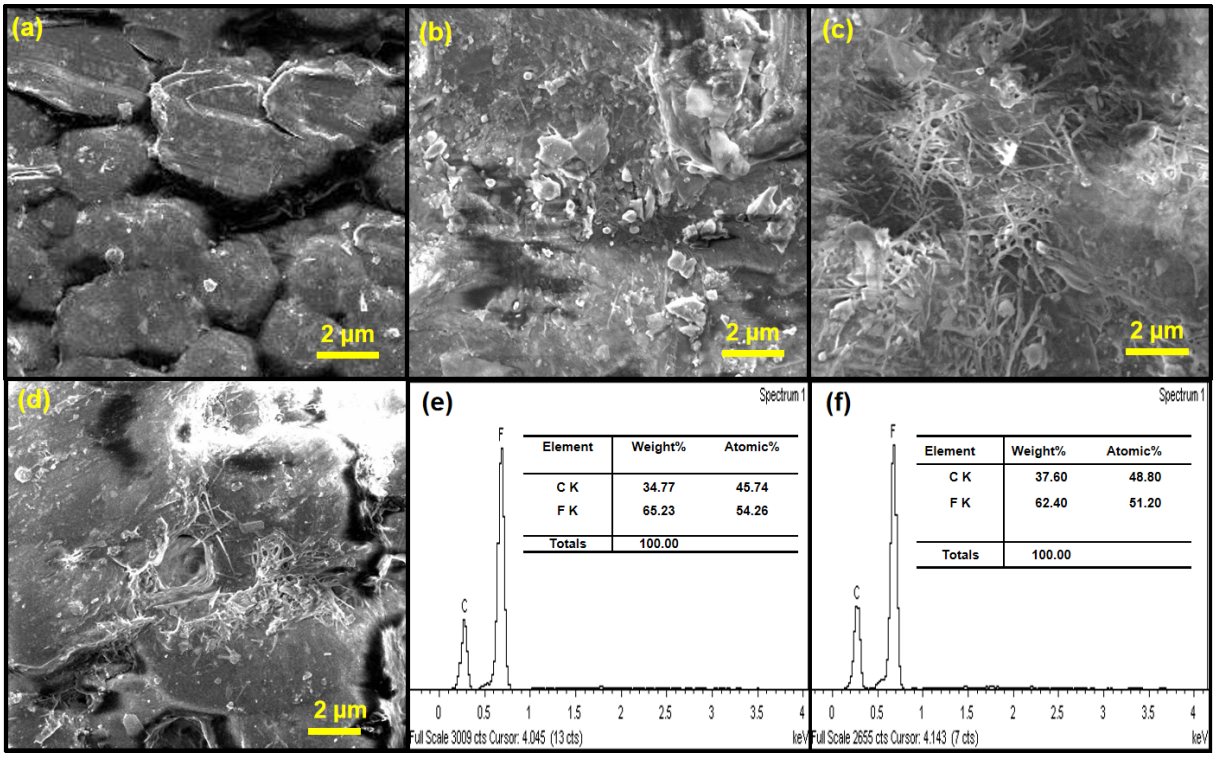


Fig. 3. FESEM images of **(A)** pure PVDF, **(B)** PVDF/G-1.0%, **(C)** PVDF/G-1.5%, **(D)** PVDF/G-2.0%, **(E)** EDX analysis of pure PVDF, and **(F)** EDX analysis of the PVDF/G composite film. EDX, energy-dispersive X-ray spectroscopy; PVDF, polyvinylidene fluoride; PVDF/G, polyvinylidene fluoride infused graphene

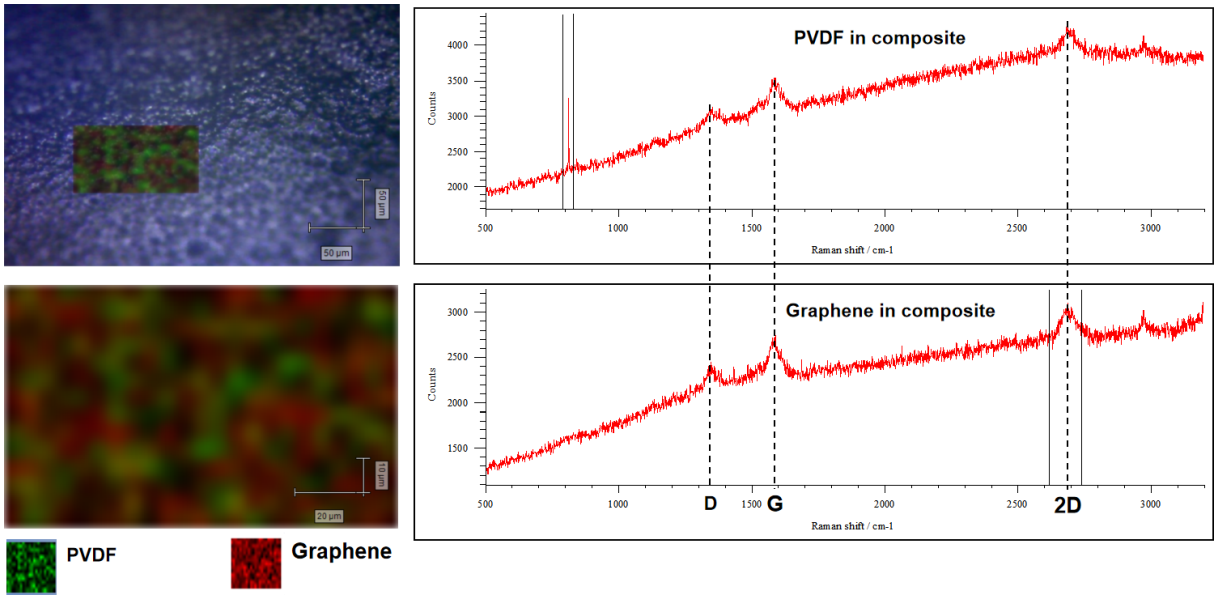


Fig. 4. Raman mapping of PVDF/G composite. PVDF/G, polyvinylidene fluoride infused graphene

significantly heightened, thus preventing the PVDF micro molecules from slipping along the graphene filler. Thus, the interpenetration of the PVDF polymer is rendered difficult, which leads to low tensile strength. Additionally, the film casting method, along with poor dispersion of filler at higher concentration, may also result in the porosity of composite with reduced tensile properties [31].

3.2. Infusion of graphene in the PVDF matrix

Figure 3 shows FESEM images of pure PVDF and PVDF/G composite with 0.5 wt.% up to 2.0 wt.% graphene loading at high magnification. As demonstrated in Figure 3A, no flaky aggregate can be observed on the surface of the pure PVDF. Meanwhile, PVDF/G composite film with 0.5 wt.% up to 2.0 wt.% graphene loading showed the morphology of flaky aggregation, which proves the infusion of graphene into the PVDF matrices [32]. Furthermore, the flaky aggregates and surface agglomeration increase as the percentage of graphene loaded into the composite increases, as shown in Figure 3B–3E. These observations indicate that the composites are infused with graphene filler [8]. Nevertheless, energy-dispersive X-ray spectroscopy (EDX) analysis was carried out to confirm the elemental composition, as shown in Figure 3E, 3F. Figure 3E represents the actual chemical composition of pure PVDF, which is 65.23 wt.% of fluorine and 34.77 wt.% of carbon. Meanwhile, after being infused with graphene, the chemical composition is 62.4 wt.% F and 37.6 wt.% C, as represented in Figure 3F, which demonstrates a slightly higher weight percentage for carbon, with an increment of 2.83 wt.%. It indicates that graphene filler is infused within the PVDF/G composite film. Thus, the EDX data are accurate in obtaining the investigated composites' elemental analysis and chemical composition. Furthermore, the absence of surface-level impurity elements other than the irregularities in morphology confirms that the PVDF/G composite is free from impurities.

Raman mapping shows the structure of the composite, as exhibited in Figure 4. The effectiveness of stress transferred from the PVDF matrix to the composite is due to well-defined graphene and PVDF matrix interactions. The graphene Raman spectrum exhibits three distinct prominent peaks at 1,350 cm^{-1}, 1,585 cm^{-1}, and 2,700 cm^{-1}. These prominent peaks appointed to the disordered graphite structure (D band), the tangential stretching mode of carbon–carbon bonds (G band), and also the crystalline graphitic material (2D band), which confirms the existence of graphene [33, 34]. The consistency of graphene peaks can be observed clearly in the PVDF/G composite. It confirms the existence of graphene in the PVDF/G composite.

3.3. Hydrophobic properties

Wettability testing is performed to study the intermolecular associations between the fluid and the composite, confirming its hydrophobic properties [35]. The stronger the fluid is attracted to the composite, the wider the spread of the fluid drop on the composite, and vice versa. Generally, the chemical composition of the composite is a crucial element to determine the wettability properties. Aside from the mechanical strength and elasticity, the effect of graphene loading in PVDF could improve the polymer's hydrophobicity [32]. Herein, assessment of the PVDF/G composite film's wettability was performed by measuring the film's water CA. Figure 5 displays the primary outcomes of the wettability tests involving measurement of the water CA of pure PVDF and PVDF/G composite.

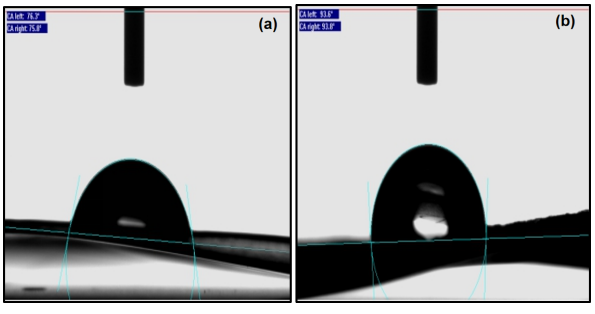


Fig. 5. Water CA of **(A)** pure PVDF and **(B)** PVDF/G composite. CA, contact angle; PVDF, polyvinylidene fluoride; PVDF/G, polyvinylidene fluoride infused graphene

The pure PVDF shows the lowest surface energy and substantial hydrophobic property, with the CA on the left and right amounting to 76.3° and 75.8°, respectively. Thus, the surface's film of pure PVDF is hydrophilic. In contrast, graphene incorporation has increased surface roughness and the water CA by 20° more than pure PVDF to 93.6° and 93.8°, respectively, for the CA on the left and right. These results indicate that the increase in hydrophobicity and fouling behavior that takes place pursuant to graphene incorporation is improved in the case of PVDF/G composite film in comparison with pure PVDF film. These significantly improved properties imply that PVDF/G composite film shows immense promise for use as an alternative antifouling biomaterial in medical applications, and that it demonstrates potential for reducing the chances of occurrences of blood clots and calcification problems.

4. Conclusions

In this work, the graphene reinforcement into the PVDF matrix strongly influences the synthesized composite's mechanical and hydrophobicity properties. The graphene reinforced PVDF was successfully achieved by solvent blending and dry-casting methods. Based on our empirical evaluation, we have ascertained that the PVDF/G-1.5 wt.% produces extremely high values for ultimate tensile stress and Young's modulus, amounting, respectively, to 90.24 MPa and 5720.88 MPa. The PVDF/G composite exhibits surface roughness and increases water CA by 20° more than pure PVDF. Based on the mechanical and hydrophobicity properties of the PVDF/G composite obtained as a result of using the solvent blending and dry-casting methods employed in the present study, it may be concluded that these methods provide an ideal processing method that can be recommended for use in future work. Therefore, the uniqueness of the PVDF/G composite promises excellent potential as a new material for biomedical applications.

Acknowledgements

The authors thank the University of Malaya for providing financial support through the Research University grants ST045-2021 and RU003-2021.

Conflict of interest

The authors declare no conflict of interest.

References

[1] Sahrash R, Siddiqa A, Razzaq H, Iqbal T, Qaisar S. PVDF based ionogels: applications towards electrochemical devices and membrane separation processes. Heliyon. 2018;4:e00847; https://doi.org/10.1016/j.heliyon.2018.e00847

[2] Tian M, Chi S, Qu L, Chen S, Ran J, Zhu S, et al. Scalable non-solvent-induced phase separation fabrication of poly(vinylidene fluoride) porous fiber with intrinsic flame-retardation and hydrophobic properties. Iran Polym J. 2018;27:115–24; https://doi.org/10.1007/s13726-017-0595-0

[3] Qu P, Zhu X, Peng X, Zhang M, Yang B, Liu, X. Ultrathin ceramic nanowires for high interface interaction and energy density in PVDF nanocomposites. Int J Appl Ceram Technol. 2019;16:1200–8; https://doi.org/10.1111/ijac.13150

[4] Kalimuldina G, Turdakyn N, Abay I, Medeubayev A, Nurpeissova A, Adair D, et al. A review of piezoelectric PVDF film by electrospinning and its applications. Sensors. 2020;20(18):5214; https://doi.org/10.3390/s20185214

[5] Saxena P, Shukla P. A comprehensive review on fundamental properties and applications of poly (vinylidene fluoride) (PVDF). Adv Compos Hybrid Mater. 2021;4:8–26; https://doi.org/10.1007/s42114-021-00217-0

[6] Abbasipour M, Khajavi R, Yousefi AA, Yazdanshenas ME, Razaghian F, Akbarzadeh A. Improving piezoelectric and pyroelectric properties of electrospun PVDF nanofibers using nanofillers for energy harvesting application. Polym Adv Technol. 2019;30:279–91; https://doi.org/10.1002/pat.4463

[7] Ruan L, Yao X, Chang Y, Zhou L, Qin G, Zhang X. Properties and applications of the β phase poly (vinylidene fluoride). Polymers. 2018;10(3):228; https://doi.org/10.3390/polym10030228

[8] Zhao X, Zhang Q, Chen D, Lu P. Enhanced mechanical properties of graphene-based poly (vinyl alcohol) composites. Macromolecules. 2010;43:2357–63; https://doi.org/10.1021/ma902862u

[9] Li C, Chen X, Luo J, Wang F, Liu G, Zhu H, et al. PVDF grafted Gallic acid to enhance the hydrophilicity and antibacterial properties of PVDF composite membrane. Sep Purif Technol. 2021;259:118127; https://doi.org/10.1016/j.seppur.2020.118127

[10] Kawai, H. The piezoelectricity of poly (vinylidene Fluoride). Jpn J Appl Phys. 1969;8:975–6; https://doi.org/10.1143/JJAP.8.975

[11] Boutouyrie P, Tropeano Anne I, Asmar R, Gautier I, Benetos A, Lacolley P, et al. Aortic stiffness is an independent predictor of primary coronary events in hyper-

tensive patients. Hypertension. 2002;39:10–5; https://doi.org/10.1161/hy0102.099031

[12] Kimoto E, Shoji T, Shinohara K, Hatsuda S, Mori K, Fukumoto S, et al. Regional arterial stiffness in patients with type 2 diabetes and chronic kidney disease. J Am Soc Nephrol. 2006;17:2245; https://doi.org/10.1681/ASN.2005101038

[13] Nilsson PM. Reducing the risk of stroke in elderly patients with hypertension. Drugs Aging. 2005;22:517–24; https://doi.org/10.2165/00002512-200522060-00005

[14] Mitchell GF. Effects of central arterial aging on the structure and function of the peripheral vasculature: implications for end-organ damage. J Appl Physiol. 2008;105:1652–60; https://doi.org/10.1152/japplphysiol.90549.2008

[15] Lederle FA, Larson JC, Margolis KL, Allison MA, Freiberg MS, Cochrane BB, et al. Abdominal aortic aneurysm events in the women's health initiative: cohort study. BMJ. 2008;337:a1724; https://doi.org/10.1136/bmj.a1724

[16] Glasser SP. Hypertension, hypertrophy, hormones, and the heart. Am Heart J. 1998;135:S16–20; https://doi.org/10.1053/hj.1998.v135.86973

[17] Aoun S, Blacher J, Safar ME, Mourad JJ. Diabetes mellitus and renal failure: effects on large artery stiffness. J Hum Hypertens. 2001;15:693–700; https://doi.org/10.1038/sj.jhh.1001253

[18] Cruickshank K, Riste L, Anderson Simon G, Wright John S, Dunn G, Gosling Ray G. Aortic pulse-wave velocity and its relationship to mortality in diabetes and glucose intolerance. Circulation. 2002;106:2085–90; https://doi.org/10.1161/01.CIR.0000033824.02722.F7

[19] Larivière R, Lebel M. Endothelin-1 in chronic renal failure and hypertension. Can J Physiol Pharmacol. 2003;81:607–21; https://doi.org/10.1139/y03-012

[20] Maitz MF. Applications of synthetic polymers in clinical medicine. Biosurf Biotribol. 2015;1:161–76; https://doi.org/10.1016/j.bsbt.2015.08.002

[21] Falde EJ, Yohe ST, Colson YL, Grinstaff MW. Superhydrophobic materials for biomedical applications. Biomaterials. 2016;104:87–103; https://doi.org/10.1016/j.biomaterials.2016.06.050

[22] Khlyustova A, Cheng Y, Yang R. Vapor-deposited functional polymer thin films in biological applications. J Mater Chem B. 2020;8(31):6588–609; https://doi.org/10.1039/D0TB00681E

[23] Liang J, Xu Y, Huang Y, Zhang L, Wang Y, Ma Y, et al. Infrared-triggered actuators from graphene-based nanocomposites. J Phys Chem C. 2009;113:9921–27; https://doi.org/10.1021/jp901284d

[24] Leenaerts O, Partoens B, Peeters FM. Water on graphene: hydrophobicity and dipole moment using density functional theory. Phys Rev B. 2009;79:235440; https://doi.org/10.1103/PhysRevB.79.235440

[25] George N, Chandra J, Mathiazhagan A, Joseph R. High performance natural rubber composites with conductive segregated network of multiwalled carbon nanotubes. Compos Sci Technol. 2015;116:33–40; https://doi.org/10.1016/j.compscitech.2015.05.008

[26] Rahman MA, Tong GB, Kamaruddin NH, Wahab FA, Hamizi NA, Chowdhury ZZ, et al. Effect of graphene infusion on morphology and performance of natural rubber latex/graphene composites. J Mater Sci Mater Electron. 2019;30:12888–94; https://doi.org/10.1007/s10854-019-01650-0

[27] Francis LF, Grunlan JC, Sun J, Gerberich WW. Conductive coatings and composites from latex-based dispersions. Colloids Surf. 2007;311:48–54; https://doi.org/10.1016/j.colsurfa.2007.08.026

[28] Balguid A, Rubbens MP, Mol A, Bank RA, Bogers AJJC, van Kats JP, et al. The role of collagen cross-links in biomechanical behavior of human aortic heart valve leaflets – Relevance for tissue engineering. Tissue Eng. 2007;13:1501–11; https://doi.org/10.1089/ten.2006.0279

[29] Mavrilas D, Missirlis Y. An approach to the optimization of preparation of bioprosthetic heart valves. J Biomech. 1991;24:331–9; https://doi.org/10.1016/0021-9290(91)90351-M

[30] Misfeld M, Sievers HH. Heart valve macro- and microstructure. Philos Trans R Soc Lond B Biol Sci. 2007;362:1421–36; https://doi.org/10.1098/rstb.2007.2125

[31] Jin SH, Park YB, Yoon KH. Rheological and mechanical properties of surface modified multi-walled carbon nanotube-filled PET composite. Compos Sci Technol. 2007;67:3434–41; https://doi.org/10.1016/j.compscitech.2007.03.013

[32] Rafiei H, Abbasian M, Yegani R. Polyvinylidene fluoride as a neat and the synthesized novel membranes based on PVDF/polyvinyl pyrrolidone polymer grafted with TiO_2 nanoparticles through RAFT method for water purification. Iran Polym J. 2021;30:769–80; https://doi.org/10.1007/s13726-021-00928-7

[33] Hanke T, Charitos EI, Stierle U, Robinson D, Gorski A, Sievers HH, et al. Factors associated with the development of aortic valve regurgitation over time after two different techniques of valve-sparing aortic root surgery. J Thorac Cardiovasc Surg. 2009;137:314–9; https://doi.org/10.1016/j.jtcvs.2008.08.006

[34] Marlinda AR, Kamaruddin NH, Fadilah AW, Said, M, Hamizi, NA, Johan, MR. Simple dispersion of graphene incorporated rubber composite for resistive pressure sensor application. Polym. Eng. Sci. 2021; 61: 1476-1484; https://doi.org/10.1002/pen.25668

[35] Verplanck N, Coffinier Y, Thomy V, Boukherroub R. Wettability switching techniques on superhydrophobic surfaces. Nanoscale Res Lett. 2007;2:577; https://doi.org/10.1007/s11671-007-9102-4

Received 2021-10-25
Accepted 2022-03-10